

Discretely tunable optical packet delays using channelized slow light

Zhimin Shi (石志敏)* and Robert W. Boyd†

The Institute of Optics, University of Rochester, Rochester, New York 14627, USA

(Received 17 September 2008; published 6 January 2009)

We describe a procedure for increasing the fractional delay (or delay-bandwidth product) of a slow-light system. A broadband input signal is sliced into several frequency bands. The light in each band propagates through a separate channel which possesses a highly reduced group velocity over a narrow frequency band. The output of each channel is then combined to form a single output field. For certain discretely distributed values of the group velocity of each channel, the output can replicate the input waveform without the need to adjust the output phase of each channel. Because this scheme makes use of many parallel channels, it can overcome a fundamental limit [D. A. B. Miller, *Phys. Rev. Lett.* **99**, 203903 (2007)] to the delay-bandwidth product for single-channel devices. A practical design is proposed using spectral slicers and stimulated Brillouin scattering as the narrow-band slow-light process. Numerical simulation shows that such a channelized slow-light element can have nearly uniform gain and group index over very large bandwidths.

DOI: 10.1103/PhysRevA.79.013805

PACS number(s): 42.25.Bs, 42.30.Lr, 42.65.Es

Recent studies of slow and fast light [1] have led to significant progress both in its conceptual understanding [2–4] and in the development of its applications [5–7]. Under many circumstances, a primary figure of merit for the evaluation of the performance of slow-light delay devices is the maximum achievable fractional delay [8] (also known as the delay-bandwidth product). This quantity gives the delay as measured in pulse widths. In practice, this quantity is often limited not by the amount by which the velocity can be reduced but rather by the maximum distortion or change in power level that a signal is allowed to acquire in passing through such a material [9].

Many schemes [10–12] have been proposed for increasing the fractional delay of many slow-light media by broadening and flattening the intrinsically narrow resonance structures. Nonetheless, there exists serious practical limits [13–15] on the maximum fractional delay that a single-channel slow-light medium can produce. Of particular interest is the Miller limit, which relates the maximum achievable fractional delay $\tau_g \Delta\nu$ (τ_g and $\Delta\nu$ being the time delay and the signal bandwidth, respectively) of a device of size L with its average refractive index n_{avg} and its maximum variation of Δn over $\Delta\nu$ near the center wavelength λ_0 through the relation [13]

$$\tau_g \Delta\nu \leq n_{\text{avg}} L \Delta n / (\sqrt{3} \lambda_0). \quad (1)$$

Channelized slow light [16–20] has recently been proposed as a procedure for improving the performance of slow-light devices based on materials with an intrinsically narrow working bandwidth. The basic idea of channelization is to create separate narrow-band slow-light spectral channels for different frequency components of a broadband signal and subsequently combine these outputs to achieve large fractional delays of broadband signals. One proposal for channelized slow light is to create multiple spectral resonances in, e.g., a photorefractive crystal [17] or an electromagnetically

induced transparency medium [19]. While such a method is capable of delaying a pulse train with discrete spectral components, it has serious distortion problems when dealing with signals with a continuous spectrum [17]. Moreover, such a method cannot exceed Miller's limit because of its one-dimensional geometry. Another type of proposal uses dispersive elements such as gratings and prisms to form a continuous span of spatially separated channels [16–18,20]. Such a treatment can effectively increase the working bandwidth, but it cannot increase the maximum fractional delay [18]. This is because the effective group index of the channelized device is reduced by the same factor as by which the working bandwidth is increased through the use of such channelization. As a result, none of the proposals of channelized slow light so far can overcome Miller's limit for a signal with a continuous spectrum.

In this paper, we propose a practical design of a channelized delay device which, by using a finite number of spatially separated channels, can overcome Miller's limit. Furthermore, we show that such a device can achieve discretely tunable optical packet delays without the need of dynamically controlling the phase of each channel.

We first review the operation of a linear, single-channel slow-light element. The transmission through such an element can be described using a frequency-domain transfer function $\mathcal{H}(\nu)$ according to the relation $E_{\text{out}}(\nu) = E_{\text{in}}(\nu) \mathcal{H}(\nu)$, where $E_{\text{in}}(\nu)$ and $E_{\text{out}}(\nu)$ are the complex amplitudes of the input and output fields, respectively. $\mathcal{H}(\nu)$ is given by

$$\mathcal{H}(\nu) = \mathcal{A}(\nu) e^{i\phi(\nu)} = \exp[i2\pi\nu\tilde{n}(\nu)L/c], \quad (2)$$

where $\mathcal{A}(\nu)$ and $\phi(\nu)$ are the amplitude and phase response functions, respectively, $\tilde{n} = n_r + in_i$ is the complex refractive index of the medium, L is the length of the medium, and c is the velocity of light in vacuum.

We consider a slow-light medium to be ideal if it possesses constant group index and gain over the signal bandwidth. In this situation, the real part of the refractive index n_r is given by (see the dotted line in Fig. 1)

*zshi@optics.rochester.edu

†boyd@optics.rochester.edu

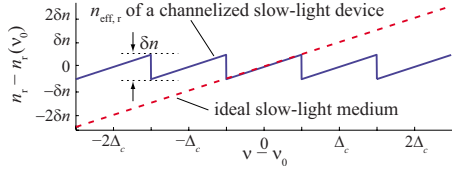


FIG. 1. (Color online) Refractive index as a function of the detuning from some center frequency ν_0 for an ideal slow-light medium and for a channelized slow-light medium. Here $\delta n = n'_g \Delta_c / \nu_0$ is the maximum refractive index variation for both types of medium within the frequency interval Δ_c .

$$n_r(\nu) = n_r(\nu_0) + \frac{n'_g}{\nu_0}(\nu - \nu_0), \quad (3)$$

where ν_0 is some center frequency, $n'_g = n_g - n_r(\nu_0)$ is the reduced group index, and $n_g = n_r + \nu dn_r/d\nu$ is the group index of the medium near ν_0 . Note that for any material medium $n_r(\nu)$ and $n_i(\nu)$ are related through the Kramers-Kronig (KK) relations, and it is thus very difficult to design an ideal slow-light medium with large n'_g and uniform n_i over a large bandwidth.

In this paper, we propose a design for channelized slow light. The input signal is first spectrally sliced into M spatially separated channels with a frequency spacing of Δ_c . The frequency components in each spectral channel then propagate through the corresponding narrow-band slow-light medium of length L before they are combined to restore a delayed output signal.

Since such a channelized device is still a linear system with single input and output ports, the transmission through the device can also be described by means of the transfer function $\mathcal{H}(\nu)$ of Eq. (2). For the ideal case in which the spectral slicing is perfect (i.e., the transmission window in each channel is of rectangular shape without any phase distortion [10]) and the slow-light medium of length L in each channel is ideal, the transfer function of such a channelized delay device is given by

$$\mathcal{H}(\nu) = \exp[i2\pi\nu\tilde{n}_{\text{eff}}(\nu)L/c], \quad (4)$$

where $\tilde{n}_{\text{eff}}(\nu)$ is the effective complex refractive index of the device and its real part $n_{\text{eff},r}(\nu)$ is given by

$$n_{\text{eff},r}(\nu) = n_{\text{eff},r}(\nu_0) + \frac{n'_g}{\nu_0}(\nu - \nu_0 - m\Delta_c), \quad (5)$$

for frequency components within the m th channel (i.e., for $|\nu - \nu_0 - m\Delta_c| < \Delta_c/2$, see also the solid line in Fig. 1). Because \tilde{n}_{eff} is not the property of a single uniform medium but rather is determined by distinct, spatially separated media for frequencies within different spectral channels, it is possible to design such a channelized delay device for which the effective group index and gain are constant over an arbitrarily large bandwidth. Note that the entire channelized element is still a causal, linear element. However, because we can use nonminimal phase filters [21] to construct the spectral slicers, the magnitude and the phase of the total transfer function $\mathcal{H}(\nu)$ of such a channelized element do not have to obey the usual Hilbert transform relations [21,22].

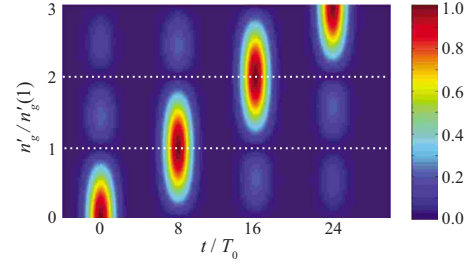


FIG. 2. (Color online) False-color representation of the amplitude of the output signal propagating through an ideal channelized delay device as a function of time and of the value of n'_g . Here the input signal is a Gaussian pulse with a half width to the $1/e$ intensity value of T_0 , and the channel spacing Δ_c is set equal to $1/(8T_0)$. The time axis is set so that $t=0$ indicates no delay as in the case in which $n'_g=0$.

One sees from Eq. (5) that the phase response function $\phi(\nu)$ is discontinuous at the boundaries of neighboring channels. The difference in the values of $\phi(\nu)$ between the two sides of any channel boundary is given by

$$\Delta\phi \approx k_0 \delta n_{\text{eff}} L = 2\pi n'_g \Delta_c L/c, \quad (6)$$

where $\delta n_{\text{eff}} = n'_g \Delta_c / \nu_0$ is the difference in the values of the effective refractive index of the device between the two sides of the channel boundary (see Fig. 1). This phase jump of $\Delta\phi$ can lead to distortion and breakup of the reconstructed output pulse, unless the output phase of each channel is actively adjusted by means of some additional phase shifter [17]. However, the transfer function $\mathcal{H}(\nu)$ becomes automatically continuous (that is, there is no need for further phase adjustment) when

$$\Delta\phi = 2\pi N, \quad (7)$$

where N is any integer. In such cases, the difference between the transfer function at one side of a channel boundary and the other is a multiplicative factor of $\exp(i\Delta\phi) = 1$. Therefore, one can achieve a delayed output signal without any distortion. For a channelized device with a fixed length L and channel spacing Δ_c , the condition of Eq. (7) indicates that the reduced group index n'_g of each channel needs to satisfy the following condition:

$$n'_g(N) = \frac{Nc}{L\Delta_c}. \quad (8)$$

Under such conditions, the transmission through the channelized delay device is equivalent to that through an ideal slow-light medium with the same length L and reduced group index $n'_g = n'_g(N)$ over the entire signal bandwidth. Thus, a distortion-free signal can be produced at the output port of the device with a group delay $\tau_g(N)$ given by

$$\tau_g(N) = \frac{n'_g(N)L}{c} = \frac{N}{\Delta_c}. \quad (9)$$

Some numerical predictions based on these considerations are displayed graphically in Fig. 2. Here we consider an input signal in the form of a Gaussian pulse and we calculate the output pulse shape through use of the transfer function of

Eq. (4). The amplitude of the output is then plotted against time on the horizontal axis and the reduced group index n'_g on the vertical axis. We see that for specific values of n'_g (see the white dotted line in Fig. 2) the output is in the form of a well defined pulse, whereas for other values of n'_g pulse breakup occurs. Since the values of n'_g that allow an undistorted output pulse are spaced discretely at integer multiples of $c/(L\Delta_c)$, the possible time delays are also distributed discretely in integer multiples of the time interval Δ_c^{-1} .

For an input signal of a bandwidth $\Delta\nu$, the number of required channels is $M=\Delta\nu/\Delta_c$. Moreover, the maximum variation in the (effective) refractive index of the channelized device is given by $\Delta n=n'_g\Delta_c/\nu_0$, which is independent of the signal bandwidth. Thus, the fractional delay can be written in terms of Δn as follows:

$$\tau_g\Delta\nu = \frac{n'_g L \Delta\nu}{c} = \frac{\Delta n \nu_0 L \Delta\nu}{\Delta_c c} = \frac{M \Delta n L}{\lambda_0}. \quad (10)$$

This equation is of similar form to the expression of Miller's limit [see Eq. (1)]. In addition to the difference of some numerical constants, our expression has a factor of M in the numerator. Since M is a free design parameter determined by the channel spacing relative to the signal bandwidth, the fractional delay of a channelized delay device is not restricted to Miller's limit. Indeed, there is no obvious limit to how large the fractional delay can become in a channelized device.

Let us next consider not a single pulse but rather a wave train (data packet) in the form of B pulses with temporal spacing of τ_b . The duration of this wave train is then of the order of $\tau_p=B\tau_b$. We want to determine the extent to which we can achieve a large fractional delay of the entire wave train. The ability to do so is important for various applications such as all-optical buffering and routing. When the condition of Eq. (8) is satisfied, the fractional delay of the entire data packet is given by

$$\frac{\tau_g(N)}{\tau_p} = \frac{n'_g(N)L}{cB\tau_b} = \frac{N}{\Delta_c B\tau_b}. \quad (11)$$

One sees that when the channel spacing Δ_c satisfies the condition

$$\Delta_c = 1/(B\tau_b), \quad (12)$$

the channelized element can achieve discretely tunable delays that are integer multiples of the time duration of the entire data packet. Crucially, no dynamic control of the phase of the output of each channel is required to achieve this control of the signal delay.

To illustrate more explicitly the promise of channelized slow-light devices, we next present a practical design for a channelized slow-light buffer for high speed telecommunication systems and we analyze its performance. We consider a signal data rate of 40 Gbps. Each "1" bit is represented by a Gaussian pulse and a "0" bit is represented by the absence of the pulse. The temporal full width at half maximum (FWHM) of the "1" bit is 12.5 ps, which is consistent with a return-to-zero (RZ) amplitude modulation format of 40 Gbps with 50% duty cycle. For illustrative purposes we consider a

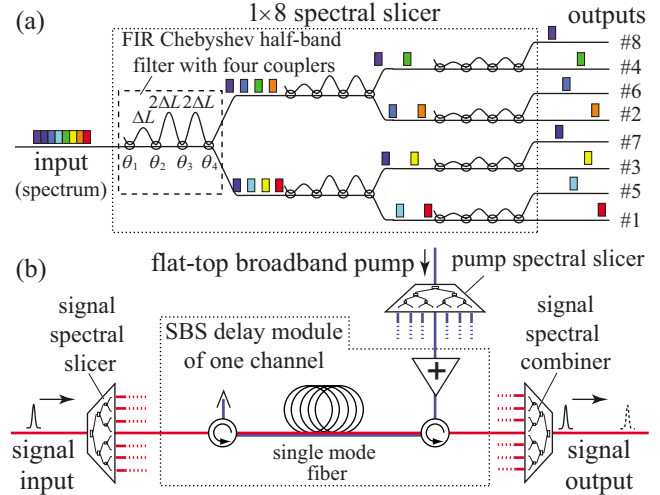


FIG. 3. (Color online) Schematic diagrams of (a) a 1×8 spectral slicer using cascaded half-band filters and (b) a channelized SBS slow-light delay element.

data packet containing 4 bits. In order to achieve packet delays, the channel bandwidth is determined, according to Eq. (12), to be $\Delta_c=10$ GHz. We choose the total number of channels to be $M=7$ to cover the entire signal spectrum [as indicated by the dotted line in Fig. 4(a)].

As an example, we construct the spectral slicer by cascading a series of flat-top finite impulse response (FIR) Chebyshev half-band filters PLEAS with 4 couplers [23] as shown in Fig. 3(a). After the spectral components in each channel are delayed, we use another spectral slicer to combine all the spectral components to restore the broadband signal. The two spectral slicers are designed to have opposite dispersions [24] so that the cascaded transfer function of the two slicers has negligible phase distortion.

We choose stimulated Brillouin scattering (SBS) as the slow-light mechanism [6,7] implemented in each spectral channel. A spool of single mode fiber is contained in each channel, and the delay is controlled by selecting the appropriate pump power for each channel. The SBS Stokes shift frequency Ω_S for the assumed operating wavelength of 1550 nm is typically 12 GHz. The SBS pump-field spectral profile for each signal channel is achieved by filtering a broadband flat-top pump field (using, e.g., current modulation [25]) through an additional spectral slicer. The schematic diagram of the channelized delay element is plotted in Fig. 3(b). For simplicity, we show the SBS delay line of only one signal channel. Note that the use of spectral slicers has associated insertion loss, which is typically frequency independent. Such losses would reduce the signal power level, which may reduce the signal-to-noise ratio when the signal is detected. However, SBS is a gain-induced slow-light process, and therefore such losses can be compensated by the SBS gain or by adding an additional amplifier module after the channelized device. Moreover, since only the frequency components within the SBS gain profile (which in our case only covers the signal bandwidth) experience the gain, the SBS process acts like a filter and may actually reduce the optical noise level outside the signal bandwidth and increase the optical signal-to-noise ratio.

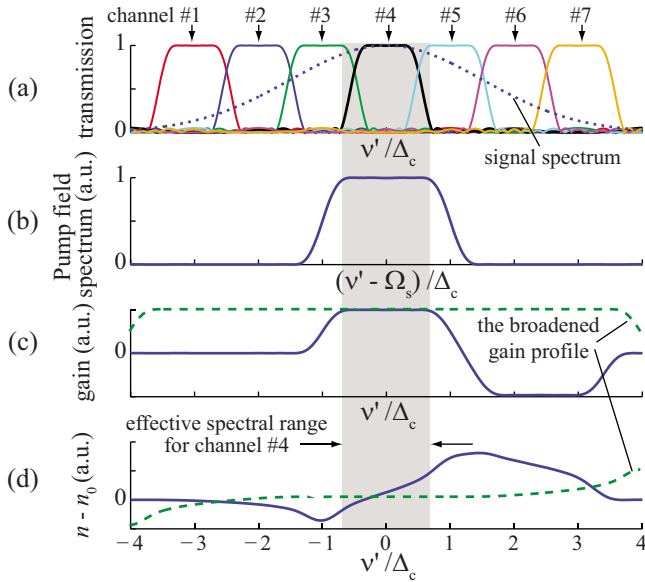


FIG. 4. (Color online) (a) Transmission of each of the seven physical signal channels of a channelized SBS delay element, (b) corresponding pump field spectrum for one particular signal channel (channel No. 4), and the SBS-induced (c) gain and (d) refractive index variation as functions of the detuning for channel No. 4 (solid line) and for a broadened gain profile (dashed line), respectively.

The transmission windows of the seven signal spectral channels are plotted in Fig. 4(a). Figure 4(b) shows the pump field profile for signal channel No. 4, and the resulting gain and refractive index as functions of frequency detuning ν' are plotted in Figs. 4(c) and 4(d), respectively. One sees that both g and n are very close to those of an ideal slow-light medium with constant group index and gain over the entire transmission window of the signal channel (see the gray region in Fig. 4).

Next, we numerically model the propagation of a wave packet containing the data stream of “1010” through the channelized delay element. For comparison, we also treat the transmission through two other types of single-channel delay elements. One is a narrow-band delay element which is equivalent to channel No. 4 of our channelized device. The other has a flat-top broadband gain profile [see the dashed lines in Figs. 4(c) and 4(d)] across the entire 70 GHz signal bandwidth, which is equivalent to the case in which the spectral channels are spatially overlapping. For the second element, we assume that the anti-Stokes SBS absorption features are compensated (e.g., using multiple pump fields [26,27]) and the signal experiences only the 70 GHz broadband gain feature.

The output waveforms for delays of 1, 2, and 3 packet lengths are plotted as the solid lines in Figs. 5(a)–5(c), respectively. One sees that our channelized delay element can achieve large packet delays with nearly no pulse distortion because it provides uniform effective group index and gain over the entire 70 GHz signal bandwidth.

The outputs of the other two types of delay elements with the same maximum (line center) CW gain are also plotted for comparison. One sees that the narrow-band single-channel delay element achieves a similar amount of delay (see the

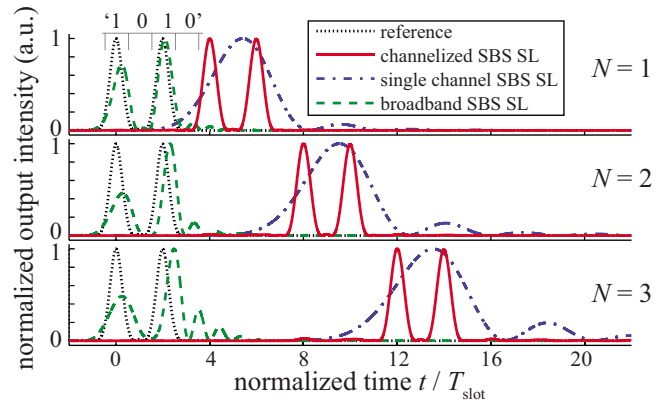


FIG. 5. (Color online) Outputs of a 40 Gbps, RZ data train “1010” after propagating through a channelized SBS delay element with Δ_c of 10 GHz (solid line), a single channel narrow-band SBS delay element (dash-dotted line), and a single channel broadband SBS delay element (dashed line), respectively. The dotted line is the reference output.

dash-dotted lines in Fig. 5) because n'_g within its working bandwidth is the same as that in our channelized element. However, because its 12 GHz working bandwidth is much less than the 70 GHz signal bandwidth, significant pulse broadening occurs at the output and the data information of “1010” is completely lost.

On the other hand, the broadband delay element possesses enough working bandwidth for the signal, but the delay is very limited (see the dashed lines in Fig. 5) because n'_g decreases significantly [see the dashed line in Fig. 4(d)] as a consequence of the broadening of the gain. Furthermore, the output signal also shows large distortion because n'_g is not uniform over the signal bandwidth.

For practical applications, it is important to evaluate the performance of our channelized delay element under the influence of imperfections. In particular, we consider the influence of phase fluctuations among the different spectral channels on the quality of the restored output signals. Such phase fluctuations can be induced by, e.g., temperature fluctuations of individual slow-light elements (fibers in our case), etc., which introduce the additional random phase $\delta\phi(m)$ to the phase response function $\phi_m(\nu)$ for the m th spectral channel.

Here we use the metric of eye opening to quantify the influences of these phase fluctuations. The eye-opening metric is defined as the maximum opening of the eye diagram (see, for example, the insets of Fig. 6), and it is closely related to the Q factor and the bit-error rate of the system [12,28–30].

We consider three different models of the channelized devices. One is an ideal device with ideal spectral slicers whose transmission windows are of rectangular shape and with ideal slow-light media that have uniform group index and zero gain. The second is a semi-ideal device with realistic spectral slicers composed of cascaded half-band filters as described above and an ideal slow-light medium in each channel. The third is the realistic model using realistic spectral slicers and SBS slow light. All three devices are set to provide one four-bit-long data packet delay.

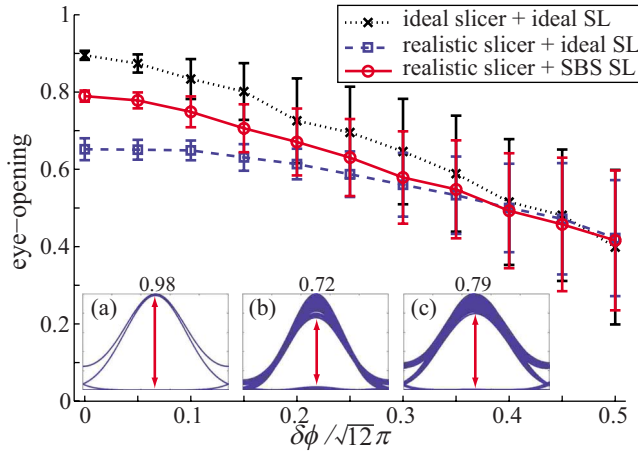


FIG. 6. (Color online) Eye openings of three channelized devices as functions of the standard deviation phase noise level $\delta\phi$ among different spectral channels. The insets show typical eye diagrams for (a) an ideal channelized slow-light device, (b) a channelized device with realistic spectral slicers and ideal slow-light media, and (c) a realistic channelized SBS slow-light device. The corresponding eye openings are given on top of each eye diagram.

For each phase noise level $\delta\phi$, we add a random phase $\delta\phi(m)$ to the phase response of the m th channel, and $\delta\phi(m)$ is uniformly distributed in the interval of $[-\sqrt{3}\delta\phi, \sqrt{3}\delta\phi]$. Note that the standard deviation of such phase noise distributions is equal to $\delta\phi$. We then calculate the eye openings of the output signal through each channelized device with an input signal of a 128-bit pseudorandom data train. The cal-

culatation is performed 200 times for each phase noise level and for each device, and the average eye openings for the three devices are plotted in Fig. 6 as functions of the phase noise level $\delta\phi$. One sees that as $\delta\phi$ increases, the eye opening gradually becomes smaller. If we require that the decrease of the eye opening due to phase fluctuations should be less than 10%, one sees from Fig. 6 that the phase noise level $\delta\phi$ should be less than approximately $\pi/(5\sqrt{12})$ (i.e., the largest phase fluctuations should be less than $\lambda/10$) for all three models. Note that since such phase fluctuations are typically slowly varying in time and independent on the fractional delay of the device, they can be compensated by, e.g., using additional low-speed phase modulators.

In summary, we have proposed a procedure for increasing the fractional delay of a slow-light system by utilizing spatially separated channels, each of which possesses a small group velocity over a narrow spectral frequency band. We have shown that by properly choosing the group index of each channel, one can achieve discretely tunable delays without the need to adjust the phase of each channel. Furthermore, we have shown that by using spatially separated channels, such a channelized device can exceed the fundamental limit of the delay-bandwidth product for a single channel device. We have proposed a practical design of such a device using spectral slicers and SBS slow light, and numerical simulation shows that discretely tunable packet delay can be achieved with minimum signal distortion.

This work was supported by the DARPA/DSO Slow Light program and by the NSF.

-
- [1] R. W. Boyd and D. J. Gauthier, in *Progress in Optics*, edited by E. Wolf (Elsevier Science, Amsterdam, 2002), Vol. 43, pp. 497–530.
- [2] S. E. Harris and L. V. Hau, *Phys. Rev. Lett.* **82**, 4611 (1999).
- [3] M. S. Bigelow, N. N. Lepeshkin, and R. W. Boyd, *Phys. Rev. Lett.* **90**, 113903 (2003).
- [4] M. S. Bigelow, N. N. Lepeshkin, and R. W. Boyd, *Science* **301**, 200 (2003).
- [5] Y. Okawachi *et al.*, *Phys. Rev. Lett.* **94**, 153902 (2005).
- [6] M. Gonzales-Herraz, K. Y. Song, and L. Thevenaz, *Appl. Phys. Lett.* **87**, 081113 (2005).
- [7] R. M. Camacho, M. V. Pack, J. C. Howell, A. Schweinsberg, and R. W. Boyd, *Phys. Rev. Lett.* **98**, 153601 (2007).
- [8] R. W. Boyd, D. J. Gauthier, A. L. Gaeta, and A. E. Willner, *Phys. Rev. A* **71**, 023801 (2005).
- [9] R. W. Boyd and P. Narum, *J. Mod. Opt.* **54**, 2403 (2007).
- [10] M. D. Stenner, M. A. Neifeld, Z. Zhu, A. M. Dawes, and D. J. Gauthier, *Opt. Express* **13**, 9995 (2005).
- [11] Z. Shi *et al.*, *Opt. Lett.* **32**, 1986 (2007).
- [12] Z. Zhu, A. M. C. Dawes, D. J. Gauthier, L. Zhang, and A. E. Willner, *J. Lightwave Technol.* **25**, 201 (2007).
- [13] D. A. B. Miller, *Phys. Rev. Lett.* **99**, 203903 (2007).
- [14] R. S. Tucker, P.-C. Ku, and C. J. Chang-Hasnain, *J. Lightwave Technol.* **23**, 4046 (2005).
- [15] J. B. Khurgin, *Opt. Lett.* **31**, 948 (2006).
- [16] Q. Sun, Y. V. Rostovtsev, J. P. Dowling, M. O. Scully, and M. S. Zubairy, *Phys. Rev. A* **72**, 031802 (2005).
- [17] Z. Deng *et al.*, *Phys. Rev. Lett.* **96**, 023602 (2006).
- [18] Z. Dutton, M. Bashkansky, M. Steiner, and J. Reintjes, *Opt. Express* **14**, 4978 (2006).
- [19] D. D. Yavuz, *Phys. Rev. A* **75**, 031801 (2007).
- [20] M. Bashkansky, Z. Dutton, F. K. Fatemi, J. Reintjes, and M. Steiner, *Phys. Rev. A* **75**, 021401 (2007).
- [21] G. Lenz, B. Eggleton, C. Giles, C. Madsen, and R. Slusher, *IEEE J. Quantum Electron.* **34**, 1390 (1998).
- [22] R. H. J. Kop, P. de Vries, R. Sprik, and A. Lagendijk, *Opt. Commun.* **138**, 118 (1997).
- [23] K. Jinguji and M. Oguma, *J. Lightwave Technol.* **18**, 252 (2000).
- [24] C.-H. Cheng *et al.* (unpublished).
- [25] A. Zadok, A. Eyal, and M. Tur, *J. Lightwave Technol.* **25**, 2168 (2007).
- [26] T. Schneider, M. Junker, and K.-U. Lauterbach, *Opt. Express* **14**, 11082 (2006).
- [27] K. Y. Song and K. Hotate, *Opt. Lett.* **32**, 217 (2007).
- [28] G. P. Agrawal, *Fiber-Optic Communication Systems*, 3rd ed. (Wiley, New York, 2002), Chap. 4.
- [29] J. Downie, *J. Lightwave Technol.* **23**, 2031 (2005).
- [30] C. Yu, T. Luo, L. Zhang, and A. E. Willner, *Opt. Lett.* **32**, 20 (2007).